HHS Public Access

Author manuscript

Lung Cancer. Author manuscript; available in PMC 2019 August 01.

Published in final edited form as:

Lung Cancer. 2018 August ; 122: 224–233. doi:10.1016/j.lungcan.2018.06.010.

Epithelial-to-Mesenchymal Transition of A549 Lung Cancer Cells Exposed to Electronic Cigarettes

Atena Zahedi[1,2], **Rattapol Phandthong**[2], **Angela Chaili**[2], **Guadalupe Lemark**[2], and **Prue Talbot**[1,2]

[1]Bioengineering Graduate Program, University of California, Riverside, California

[2]Department of Molecular, Cell and Systems Biology, University of California, Riverside, California.

Abstract

Objectives: Epithelial-to-mesenchymal transition (EMT) is the initial step enabling the metastasis of cancer cells, which often leads to death. Although smoking is a major risk factor for lung cancer, there is still widespread use of conventional cigarettes. Recently, the tobacco industry has been transformed by the introduction of electronic cigarettes (ECs), which have lower levels of carcinogens and may provide a safer alternative. Here, we investigate the ability of EC liquids and aerosols to induce an EMT in A549 lung cancer cells.

Materials and Methods: Human adenocarcinoma alveolar basal epithelial cells (A549) were exposed to EC liquids and aerosols from a popular product for 3–8 days. Live cell imaging, EMT biomarker analysis, and machine learning/image processing algorithms were used to characterize changes associated with EMT.

Results: Long-term exposure of A549 cells to menthol or tobacco-flavored EC liquids or aerosols induced an EMT that was characterized by acquisition of a fibroblast-like morphology, loss of cellto-cell junctions, internalization of E-cadherin, increased motility, and upregulation of

Corresponding author: Prue Talbot, Department of Molecular, Cell and Systems Biology, University of California, Riverside, CA. 92521, Telephone: 951-850-7783, talbot@ucr.edu.

Author Contributions: Dr. Talbot had full access to all the data in the study and takes responsibility for the integrity of the data and the accuracy of the data analysis.

Concept and design: Zahedi and Talbot

Acquisition of data: Zahedi

Analysis and interpretation of data: All authors.

Drafting of the manuscript: Zahedi and Talbot

Critical revision of the manuscript for important intellectual content: All authors.

Obtained funding: Talbot

Administrative, technical, or material support: Talbot

Supervision: Talbot

Conflict of Interest Disclosures: All authors have completed and submitted the ICMJE Form for Disclosure of Potential Conflicts of Interest and none were reported.

Disclaimer: This content is solely the responsibility of the authors and does not necessarily represent the official views of the National Institutes of Health or the FDA.

EMT markers. The EMT was concurrent with plasma membrane to nuclear translocation of active β-catenin.

Conclusion: This is the first known study to show an EMT of lung cancer cells during exposure to EC products. Because an EMT is an initial step leading to metastasis, an intractable problem that often leads to patient death, this critical finding has significant implications for former or heavy cigarette smokers who are using EC and may be at risk for lung cancer or who may already have a lung tumor.

Keywords

Electronic cigarette; Tobacco products; Metastasis; Lung cancer; Epithelial-to-mesenchymal transition; β-catenin

1. Introduction

Metastasis is a multi-step process in which cancer cells undergo an epithelial-to-mesenchymal transition (EMT), then detach from the primary tumor, and migrate to neighboring or distant organs, where they can create new tumors [1]. Once cancer cells have metastasized, treatment becomes very difficult, and the chances of survival are diminished [2]. Lung cancer accounts for the highest number of cancer-related deaths, most of which are due to the metastasis of tumor cells [3,4].

Tobacco use is the main risk factor for lung cancer and is responsible for approximately 22% of cancer-related deaths globally [5]. Cigarette smoke promotes metastasis through induction of an EMT in existing airway epithelial tumors by down-regulating epithelial cadherin (E-cadherin), which leads to loss of cell–cell adhesion and apical–basal polarity [6–8].

Electronic cigarettes (EC) are tobacco products that have rapidly gained worldwide acceptance and are often promoted as harm-reduction or smoking-cessation alternatives [9]. Their introduction into world markets has come without much prior research on their potential to cause cancer or effect cancer progression. Prior in vitro studies on EC have focused on their toxicity [10,11], with one recent in vitro study showing that EC aerosol produced little mutagenicity [12]. These studies were all done over relatively short exposure periods, usually lasting only 24–48 hours. Other studies demonstrated that EC exposure resulted in carcinogenic transformation in *Salmonella typhimurium* [13] and DNA damage in a rat lung model [14] and mouse organs [15].

No study to date has examined the potential for EC to cause an EMT and contribute to the progression of a pre-existing tumor. In this study, we tested the hypothesis that longer exposures of lung cancer cells to EC liquids and aerosols, typical of those EC users receive, induces an EMT, thereby creating the potential for metastasis.

2. Materials and Methods

2.1 EC liquids and aerosols

Menthol and tobacco flavors of a leading cartomizer style EC were purchased at local markets in Southern California. Product boxes were labeled to contain propylene glycol, glycerol, and nicotine (48 mg/ml). Flavor chemicals were not listed on product packaging but were presumed to be present to impart menthol and tobacco flavor. Liquids were removed from cartomizers by centrifugation, and 1% dilutions by volume were prepared in A549 culture medium. Aerosols were generated using a smoking machine by taking 4.3 sec puffs (average for EC users) every 1 minute with an adjusted flow rate to produce a consistent robust puff. Aerosols were collected in A549 culture medium in a 250 mL round-bottom flask, which was suspended in an ethanol and dry ice bath to allow immediate condensation and capture of aerosol puffs. After collection, medium was warmed to room temperature, aliquoted, then immediately frozen and stored at - 80°C until used. Six puffs were dissolved per 1 mL of A549 culture medium, which is referred to as 6 total-puff-equivalents (TPE) of aerosol. Both e-liquids and aerosols were passed through a 0.2μm filter before use in experiments.

2.2 Long-term culturing of A549 lung cancer cells

A549 CCL-185 cells (ATCC, Manassas, VA USA), which were previously derived from a human lung adenocarcinoma, were grown on non-coated T-25 flasks and cultured in ATCC F-12 K medium with 10% A549-specific fetal bovine serum in 5% CO_2 at 37°C. Cells were incubated in control medium or medium containing dilutions of aerosol or EC liquid until 80% confluent, then passaged using 0.25% trypsin, and grown in control or treatment medium for 3–8 days.

2.3 Morphological analysis

Cell morphology was classified as cobblestone (normal morphology), enlarged, or elongated using CL-Quant (DR Vision, Seattle WA) and CellProfiler image processing software [16] and a custom machine learning algorithm written in MATLAB software (MathWorks Natick, MA, USA). Each image was segmented using CL-Quant software and manually modified to separate individual cells. The binary image of the segmentation was exported into CellProfiler to extract 61 morphological features from which six (area, compactness, eccentricity, major axis length, minor axis length, and solidity) were used to develop a learning library. A library consisting of 126 cells was manually classified to provide ground truth for the three morphological classes. Next, 10-fold cross-validation was conducted resulting in 97% accuracy in classification. Three separate (untrained) datasets consisting of 359 cells were run through the supervised machine learning algorithm and were validated manually, resulting in 89% accuracy. Datasets presented in this paper were automatically analyzed using this classifier.

2.4 Immunocytochemistry

Immunocytochemistry was performed using antibodies to EMT markers that included E-cadherin and vimentin (Millipore, Burlington, MA, USA), N-cadherin (R&D Systems,

Minneapolis, MN, USA), metalloproteinase 9 (MMP9) and P120 (Abcam, Cambridge, MA, USA), and active (non-phosphorylated) β-catenin (Cell Signaling, Danvers, MA, USA). Also, an early endosome antigen 1 (EEA1) antibody (Cell Signaling, Danvers, MA, USA) was used for the E-cadherin colocalization study. Briefly, cells were grown in Ibidi chamber slides (Ibidi, Munich, Germany) and fixed using 4% paraformaldehyde. Cells were blocked in 10% donkey serum (Sigma-Aldrich, St. Louis, MO, USA) in 0.1% Triton-X (Bio-Rad, Hercules, CA, USA) in PBS, and primary antibodies were diluted in 0.2% Tween (Sigma-Aldrich, St. Louis, MO, USA) in PBS and incubated at 4°C overnight. Cells were next washed in PBS then incubated in Alexa Fluor 594 and 488 secondary antibodies (Life Technologies, Eugene OR USA) at room temperature for 1 hour, then mounted in Vectashield (Vector Laboratories, Burlingame, CA USA).

2.5 E-cadherin transfection and internalization

For the E-cadherin/EEA1 co-localization study, cells were first transfected with an E-cadherin-GFP plasmid (Addgene #28009, Cambridge, MA USA). Briefly, cells were plated the day before transfection, a DNA-In A549 transfection reagent was used (MTI-GlobalStem, Gaithersburg, MD USA), and cells were incubated for 18–24 hours to allow gene expression. Next, the transfected cells were trypsinized and re-plated with EC liquids or aerosol for 4 days. Lastly, cells were immuno-labeled with an early endosome marker, EEA1, to demonstrate co-localization and internalization of E-cadherin into endocytic vesicles.

To confirm co-localization of E-cadherin and EEA1, a line scanning method was used. Briefly, intensity data for representative images in Figures 4A-E were collected by the line intensity tool in Nikon Elements Advanced Research software (Nikon Instruments, Melville, NY). Lines with a relative length equivalent to 35 μm were drawn on representative images. Pixel intensity data were collected along the line from both green (E-cadherin) and red (EEA1) channels. To rescale intensity data to a 0 to 1 range, raw intensity data were normalized with the feature scaling equation:

$$z_i = \frac{x_i - \min(x)}{\max(x) - \min(x)}$$

where z_i represents the normalized intensity value, which was computed using min and max intensity values in the set x. x_i represents the intensity value before normalization. Normalized intensity values were plotted using GraphPad Prism.

2.6 Fluorescence and phase contrast microscopy

Time-lapse fluorescent images were collected using an inverted Eclipse Ti-E microscope (Nikon Instruments, Melville, NY) equipped with a 60X objective (numerical aperture 0.85) and captured on the high-resolution Andor Zyla VSC-04941 camera (Andor, Belfast, UK). The live cells were placed in a LiveCell incubation chamber (Pathology Devices Inc., San Diego CA USA), which were kept at 37°C, 5% CO_2, and 90% relative humidity. The images were de-convoluted using the Live De-blur setting in the Nikon NIS Elements software. Fluorescence analysis was quantified using CL-Quant software (DR Vision, Seattle, WA)

and CellProfiler. Phase contrast time-lapse videos of A549 cells were captured in a BioStation CT Incubator (Nikon Instruments, Tokyo, Japan).

2.7 Motility and Migration Analysis

Phase contrast and Hoechst 33342 (ImmunoChemistry Technologies, Bloomington, MN USA) fluorescent time-lapse images were captured every 15 minutes using a BioStation CT. CL-Quant software was used to track and extracted motility information. First, the tophat preprocessing method was used to remove noise and strengthen the signal in the Hoechst (blue) channel (excitation 350nm). Small object removal and background subtraction procedures were applied to minimize background noise. The tracking procedure was applied to the final signal segmentation to create trajectory tracks for cells with fluorescent signal. Tracking data were exported to Excel and imported into MATLAB to generate migratory graphs, which displayed the total length traveled and the initial-final position displacement for each cell. Motility of control and treated cells was also compared using the wound healing assay, as described preciously [17]. Three independent experiments were done for each parameter studied, and statistical analyses were done using one-way ANOVAs with Prism (GraphPad, San Diego, CA USA) and Minitab software (State College, PA USA).

2.8 Quantification of active β-catenin

Active β-catenin and P120 were visualized using immunocytochemistry and nuclei were labeled with DAPI-Vectashield (Vector Laboratories, Burlingame, CA USA). For the β-catenin (red channel) signals, images were first smoothed to normalize uneven pixel distribution and rescaled to stretch the fluorescence signal from 0 to 1. Tophat and bottomhat methods were used to enhance the signal, and adaptive MOG (mixture of Gaussian) thresholding was applied to remove noise (Supplementary Methods). Otsu's method was used to segment and extract fluorescent β-catenin signals [18]. Active β-catenin and nuclei segmentations were co-localized. The percent of active β-catenin counts or area inside the nucleus was calculated by dividing the co-localized signal by the total β-catenin signal. For both area and count data, statistical analyses were done on arcsine transformed percent data using a one-way ANOVA with Dunnett's post hoc test, in which treated groups were compared to the control.

2.8 Quantification of P120 internalization

P-120 images were imported into CL-Quant for analysis. Tophat was used to remove background noise (Supplementary Methods). P120 signals were segmented using the global threshold method. At the tight junction, P120 signals were band-like, whereas internalized P-120 was punctate. Segmented small puncta were filtered out based on size. The remaining larger objects were then "skeletonized" as described in the CL-Quant instruction manual to enhance the band-like morphology and remove non-band-like objects. The skeletons were overlaid on the original segmentation and used to separate P-120 signals at tight junctions from internalized signal. Counts and area information were extracted from both signals. One-way ANOVAs with Dunnett's post hoc test were performed on the data. Treated groups were compared to the control group.

3. Results

3.1 EC E-liquids and aerosols induce morphological changes consistent with an EMT

A549 cells normally grow as tightly adhering “cobblestone” monolayers with a few elongated and large cells interspersed among the cobblestone cells (Fig. 1A). The relative abundance of each cell type was evaluated using a custom protocol developed with Cl-Quant, CellProfiler, and MATLAB software. By 3–4 days of treatment with e-liquid or aerosol, there was a significant decrease in the cobblestone cells and a corresponding increase in single elongated mesenchymal-like cells, consistent with an EMT (Figs. 1A-D). There was also an increase in enlarged cells, which were more pronounced in the e-liquid treatments (Figs. 1B, 1D) and often multinucleated (Supplementary Fig. 1). In time-lapse videos, e-liquid and aerosol treated cells frequently contacted but did not adhere to neighboring cells, whereas control cells formed tight cell-to-cell connections with each other (Figs. 1E-G). In Figures 1E-G, each individual cell was numbered, and the progeny were followed over time.

3.2 Molecular Markers of an EMT

To confirm that the above changes were due to an EMT, molecular markers characteristic of cells transitioning from an epithelial-to-mesenchymal phenotype were used. Cancer cellproduced MMP9 is required for invasion through the extracellular matrix during metastasis [19]. MMP9 was upregulated by day 4 in A549 cells treated with either e-liquid or aerosol (Figs. 2A, 2C). By 8 days of treatment, E-cadherin was lost from the cell surface (Fig. 2B), consistent with the observed lack of cell-to-cell adhesion (Figs. 1E-G). Immunocytochemistry also revealed an increase in total vimentin after both 4 days (Supplementary Fig. 2 A-C) and 8–9 days of exposure (Figs. 2B, 2D integrated density) and an increase in vimentin cross points at day 8, indicative of increased filament density (Fig. 2E). Vimentin is overexpressed in epithelial cancers undergoing an EMT and facilitates accelerated tumor growth and invasion [20]. These changes in vimentin likely facilitate the transition of cells to a more elongated phenotype. In addition, N-cadherin, another marker for an EMT, was also increased in cells exposed to EC products (Supplementary Fig. 3). These molecular marker data collectively support the idea that EC treated cells undergo an EMT during 4–8-days of exposure.

3.3 Internalization of E-cadherin during the EMT

One of the primary modes of EMT initiation is the reduction of membrane E-cadherin via the endocytic machinery. To assess whether the decrease in E-cadherin expression at the cell membrane was due to its internalization, 4 day-treated A549 cells were transfected with an E-cadherin plasmid and then immuno-labeled with an early endosome marker (EEA1). The control cells revealed very few co-localized signals; whereas both the menthol and tobacco e-liquid and aerosol treated groups had distinct co-labeled puncta indicative of internalized E-cadherin cargo (Figs. 3A-F). Accumulation of E-cadherin was seen in the perinuclear region (Fig. 3C, white arrow)

3.4 Treatment with EC liquid and aerosol increased cell motility

An increase in cell motility is characteristic of cancer cells undergoing an EMT [1]. To determine if EC-treatment enhanced cell migration, A549 cells were labeled with the Hoechst 33342 live cell nuclear dye and monitored over time in a BioStation CT. A dual fluorescence and phase contrast tracking algorithm was developed to monitor the motility of each cell. Cells treated with e-liquids and aerosols for 3–4 days showed an increase in the population of motile cells (total distance traveled > 30 μm) (Figs. 4A-E). Migration graphs also showed that control cells mainly exhibited a random-walk (Brownian) type motion, whereas most of the treated cells exhibited a "directed" movement (Figs. 4A-C). The increase in cell motility was confirmed using the wound healing or scratch assay. Again, both the e-liquid and aerosol treated cells showed significantly greater motility than untreated controls (Supplementary Fig. 4).

3.5 Translocation of active β-catenin and P120 from the plasma membrane to the cytoplasm and nucleus

Immunocytochemistry was performed to compare the localization of β-catenin and P120, two adherens junction proteins important in cell polarity, in the control and treated groups. In treated cells, the active form of β-catenin showed a marked decrease in cell junctions and a corresponding increase inside the cells (Fig. 5A). If de-phosphorylated (active), β-catenin is stabilized and protected against degradation by GSK-3β and can move into the nucleus to initiate transcription. Image processing software was used to quantify co-localization of active β-catenin with the nuclear DAPI-stain. A significant increase in the number and area (%) of β-catenin puncta in the nucleus was observed in treated cells (Figs. 5B-C). Treatment of A549 cells with e-liquid or aerosol caused a decrease in P120 at the cell membranes after 3–5 days of treatment (Fig. 5D) and an increase in cytoplasmic levels (percent of P120 internalized by area and count shown in Figs. 5E and 5F respectively). Unlike β-catenin, P120 did not show an accumulation in the nuclei of aerosol treated groups (Fig. 5D), and therefore was not quantified.

4. Discussion

Previous *in vitro* studies with normal and cancer lung cells have generally used short-term exposures to EC fluids or aerosols [21]. These studies have shown various effects including decreased metabolic activity often accompanied by cell death [10,11,22–24], increased inflammation [25], oxidative stress [26], DNA damage [18], and mitochondrial stress [27]. The current study is the first to examine 4–8-day exposure of cancer cells to EC liquids and aerosols and to report that such exposure causes changes in cell morphology, cell-to-cell adhesion, molecular markers, and motility consistent with an EMT. These changes include transformation of cobblestone monolayers to mesenchymal-like cells, decreased E-cadherin, increased vimentin and MMP9, and increased cell motility. There was also an increase in the number of cells with an enlarged phenotype, consistent with a case report in which a lung biopsy from an EC user had multinucleated giant cells [28]. An EMT was induced in A549 cells by both the menthol and tobacco flavored EC liquids and aerosols from the leading product of EC used in this study. This shows that the factor(s) causing the EMT is present in the fluid before heating and is not a chemical produced as a result of aerosolization. EC

users do sometimes draw e-liquid into their mouths and get e-liquid on their skin. Although not a topic in this study, there is a possibility that a similar EMT would occur in tumors localized in these tissues as well.

The EC-induced EMT was characterized by the internalization of E-cadherin via endocytosis into early endosomes with subsequent accumulation in the perinuclear region, which may be the endocytic recycling compartment (ERC) [29]. Loss of E-cadherin from junctional complexes is a ubiquitous feature of an EMT and a necessary step that enables subsequent cell migration away from a tumor during metastasis [1]. We also observed enhanced migration of cells that were no longer able to adhere to other cells.

EC treatment also resulted in the translocation of active β-catenin and P120 catenin from the plasma membrane to the cytoplasm, and β-catenin was further translocated to the nucleus. β-catenin and P120 are essential components of the cadherin-based adherens junctions, and their cytoplasmic accumulation likely contributes to the destabilization of cell junctions. Other studies have shown that the transport of these catenins to the nucleus activates Wnt-signaling (β-catenin) and Rho GTPase (P120) pathways, which in turn contribute to an EMT [29,30]. The appearance of β-catenin in the nucleus following EC liquid or aerosol treatment suggests that the EMT observed in our study was further activated by the Wnt/β-catenin pathway.

An EMT is a critical initiation step in the metastasis of lung cancer cells [1]. During an EMT, epithelial cells lose their polarity, cell-cell junctions, and cell-matrix adhesions, allowing them to migrate and invade other tissues, often remote from the primary tumor [1]. A549 adenocarcinoma cells are part of the non-small cell lung cancer (NSCLC) group. Once such cells have undergone an EMT and metastasized in patients, treatment is difficult and survival rates are very low [31].

ECs are often promoted as harm reduction products, and Public Health England has stated that they are 95% safer than conventional cigarettes [32]. These claims are often based on the observation that EC aerosols have fewer chemicals than conventional cigarettes and harmful chemicals are usually lower in concentration in ECs [33]. However, most work done on cell and animal responses to EC aerosol have not to-date looked for metastasis. One recent paper describes the formation of tumors in rat lungs exposed to EC aerosol [14]. Our data are the first to show an EMT in human lung cancer cells, a critical observation that suggests EC might lead to metastasis of existing tumors. While additional work will be required to determine if a similar EMT occurs in humans using EC, our data demonstrate an important need for additional information on this topic.

Conventional cigarette constituents induce tumor formation and contribute to cancer progression by initiating an EMT [7,8,19,34–36]. The effects induced by EC liquids and aerosols are similar to those reported for cigarette smoke, which include morphological changes, increased migratory behavior, and initiation of EMT signaling pathways. This again calls into question the safety of ECs and raises concerns about their designation as harm reduction products.

The aerosol concentration used in our study corresponds to what a user would receive while inhaling 6 puffs of EC aerosol. Although puffing topography varies with each individual [37], an average user puffs roughly 175 times/day [38]. While our work was done using continuous exposure over multiple days, the concentration of aerosol during our exposures was less than the total exposure an EC user would receive in a day (6 TPE vs 175 puffs/day). It will be important in future to mimic human inhalation of EC aerosol with in vitro models that use intermittent air liquid interface exposure.

It is not yet known if this EC produces an EMT in other types of tumor cells from the lung or other organs, and this will be an important topic for future work. Since the EMT was observed with a leading EC product, the number of users who could potentially be impacted is high. This critical finding has significant implications for dual EC users or former cigarette users who have switched to EC and may be at risk for lung cancer or who may already have a lung tumor. For EC users with no existing cancer (e.g., young users), there are also significant implications such as the loss of cell junctions in normal epithelial cells which could lead to a leaky epithelial barrier in the lung and increased permeability. This could in turn lead to inflammation, chronic obstructive pulmonary disease, and acute lung injury [39]. Given these findings, it would be advisable for health care workers to include EC use in patient medical records, particularly those with a history of cigarette smoking or dual use of EC and tobacco cigarettes. Our data warn that caution should be exercised when using EC given their ability to induce an EMT in a cancer cell line. These data bring to focus the overall need for better understanding of the effects of ECs on health, particularly with respect to cancer progression. This study further supports the 2016 Surgeon General's conclusion that EC aerosol is not harm-free [9] and that the FDA may need to regulate ECs under its authority.

Supplementary Material

Refer to Web version on PubMed Central for supplementary material.

Acknowledgments

Funding/Support: Research reported in this publication was supported by the National Institute on Drug Abuse of the National Institutes of Health under Award Numbers R01DA036493 and R21DA037365.

Role of the Funder/Sponsor: The study funder had no role in the design and conduct of the study; collection, management, analysis, and interpretation of the data; preparation, review, or approval of the manuscript; or decision to submit the manuscript for publication.

References

[1]. Lambert AW, Pattabiraman DR, Weinberg RA, Emerging Biological Principles of Metastasis, Cell. 168 (2017) 670–691. doi:10.1016/j.cell.2016.11.037. [PubMed: 28187288]

[2]. Chirieac L, Biology of Lung Cancer Metastases, in: Precis. Mol. Pathol. Lung Cancer, 2018: pp. 199–211. doi:10.1007/978-3-319-62941-4_16.

[3]. Stewart BW, Wild CP, World cancer report 2014, World Heal. Organ (2014) 1–2. doi:9283204298.

[4]. Spano D, Heck C, De Antonellis P, Christofori G, Zollo M, Molecular networks that regulate cancer metastasis, Semin. Cancer Biol 22 (2012) 234–249. doi:10.1016/j.semcancer.2012.03.006. [PubMed: 22484561]

[5]. Forouzanfar MH, Afshin A, Alexander LT, Biryukov S, Brauer M, Cercy K, Charlson FJ, Cohen AJ, Dandona L, Estep K, Ferrari AJ, Frostad JJ, Fullman N, Godwin WW, Griswold M, Hay SI, Kyu HH, Larson HJ, Lim SS, Liu PY, Lopez AD, Lozano R, Marczak L, Mokdad AH, Moradi-Lakeh M, Naghavi M, Reitsma MB, Roth GA, Sur PJ, Vos T, Wagner JA, Wang H, Zhao Y, Zhou M, Barber RM, Bell B, Blore JD, Casey DC, Coates MM, Cooperrider K, Cornaby L, Dicker D, Erskine HE, Fleming T, Foreman K, Gakidou E, Haagsma JA, Johnson CO, Kemmer L, Ku T, Leung J, Masiye F, Millear A, Mirarefin M, Misganaw A, Mullany E, Mumford JE, Ng M, Olsen H, Rao P, Reinig N, Roman Y, Sandar L, Santomauro DF, Slepak EL, Sorensen RJD, Thomas BA, Vollset SE, Whiteford HA, Zipkin B, Murray CJL, Mock CN, Anderson BO, Futran ND, Anderson HR, Bhutta ZA, Nisar MI, Akseer N, Krueger H, Gotay CC, Kissoon N, Kopec JA, Pourmalek F, Burnett R, Abajobir AA, Knibbs LD, Veerman JL, Lalloo R, Scott JG, Alam NKM, Gouda HN, Guo Y, McGrath JJ, Charlson FJ, Erskine HE, Jeemon P, Dandona R, Goenka S, Kumar GA, Gething PW, Bisanzio D, Deribew A, Darby SC, Ali R, Bennett DA, Jha V, Kinfu Y, McKee M, Murthy GVS, Pearce N, Stöckl H, Duan L, Jin Y, Li Y, Liu S, Wang L, Ye P, Liang X, Azzopardi P, Patton GC, Meretoja A, Alam K, Borschmann R, Colquhoun SM, Weintraub RG, Szoeke CEI, Ademi Z, Taylor HR, Wijeratne T, Batis C, Lozano R, Barquera S, Campos-Nonato IR, Contreras AG, Cuevas-Nasu L, De V, Gomez-Dantes H, Heredia-Pi IB, Medina C, Mejia-Rodriguez F, Montañez Hernandez JC, Razo-García CA, Rivera JA, Rodríguez-Ramírez S, Sánchez-Pimienta TG, ServanMori EE, Shamah T, Mensah GA, Hoff HJ, Neal B, Driscoll TR, Kemp AH, Leigh J, Mekonnen AB, Bhatt S, Fürst T, Piel FB, Rodriguez A, Hutchings SJ, Majeed A, Soljak M, Salomon JA, Thorne-Lyman AL, Ajala ON, Bärnighausen T, Cahill LE, Ding EL, Farvid MS, Khatibzadeh S, Wagner GR, Shrime MG, Fitchett JRA, Aasvang GM, Savic M, Abate KH, Gebrehiwot TT, Gebremedhin AT, Abbafati C, Abbas KM, Abd-Allah F, Abdulle AM, Abera SF, Melaku YA, Abyu GY, Betsu BD, Hailu GB, Tekle DY, Yalew AZ, Abraham B, Abu-Raddad LJ, Adebiyi AO, Adedeji IA, Adou AK, Adsuar JC, Agardh EE, Rehm J, Badawi A, Popova S, Agarwal A, Agrawal A, Ahmad A, Akinyemiju TF, Schwebel DC, Singh JA, Al-Aly Z, Aldhahri SF, Altirkawi KA, Terkawi AS, Aldridge RW, Tillmann T, Alemu ZA, Tegegne TK, Alkerwi A, Alla F, Guillemin F, Allebeck P, Rabiee RHS, Fereshtehnejad SM, Kivipelto M, Carrero JJ, Weiderpass E, Havmoeller R, Sindi S, Alsharif U, Alvarez E, Alvis-Guzman N, Amare AT, Ciobanu LG, Taye BW, Amberbir A, Amegah AK, Amini H, Karema CK, Ammar W, Harb HL, Amrock SM, Andersen HH, Antonio CAT, Faraon EJA, Anwari P, Ärnlöv J, Larsson A, Artaman A, Asayesh H, Asghar RJ, Assadi R, Atique S, Avokpaho EFGA, Awasthi A, Ayala BP, Bacha U, Bahit MC, Balakrishnan K, Barac A, Barker-Collo SL, del Pozo-Cruz B, Mohammed S, Barregard L, Petzold M, Barrero LH, Basu S, Del LC, Bazargan-Hejazi S, Beardsley J, Bedi N, Beghi E, Sheth KN, Bell ML, Huang JJ, Bello AK, Santos IS, Bensenor IM, Lotufo PA, Berhane A, Wolfe CD, Bernabé E, Roba HS, Beyene AS, Hassen TA, Mesfin YM, Bhala N, Bhansali A, Biadgilign S, Bikbov B, Bjertness E, Htet AS, Boufous S, Degenhardt L, Resnikoff S, Calabria B, Bourne RRA, Brainin M, Brazinova A, Majdan M, Shen J, Breitborde NJK, Brenner H, Schöttker B, Broday DM, Brugha TS, Brunekreef B, Kromhout H, Butt ZA, van Donkelaar A, Martin RV, Cárdenas R, Carpenter DO, Castañeda-Orjuela CA, Castillo J, Castro RE, Catalá-López F, Chang J, Chiang PP, Chibalabala M, Chimed-Ochir O, Jiang Y, Takahashi K, Chisumpa VH, Mapoma CC, Chitheer AA, Choi JJ, Christensen H, Christopher DJ, Cooper LT, Crump JA, Poulton RG, Damasceno A, Dargan PI, das Neves J, Davis AC, Newton JN, Steel N, Davletov K, de Castro EF, De D, Dellavalle RP, Des DC, Dharmaratne SD, Dhillon PK, Lal DK, Zodpey S, Diaz-Torné C, Dorsey ER, Doyle KE, Dubey M, Rahman MHU, Ram U, Singh A, Yadav AK, Duncan BB, Kieling C, Schmidt MI, Elyazar I, Endries AY, Ermakov SP, Eshrati B, Farzadfar F, Kasaeian A, Parsaeian M, Esteghamati A, Hafezi-Nejad N, Sheikhbahaei S, Fahimi S, Malekzadeh R, Roshandel G, Sepanlou SG, Hassanvand MS, Heydarpour P, Rahimi-Movaghar V, Yaseri M, Farid TA, Khan AR, Farinha CSES, Faro A, Feigin VL, Fernandes JG, Fischer F, Foigt N, Shiue I, Fowkes FGR, Franklin RC, Garcia-Basteiro AL, Geleijnse JM, Jibat T, Gessner BD, Tefera W, Giref AZ, Haile D, Manamo WAA, Giroud M, Gishu MD, Gishu MD, Martinez-Raga J, Gomez-Cabrera MC, Gona P, Goodridge A, Gopalani SV, Goto A, Inoue M, Gugnani HC, Gupta R, Gupta R, Gutiérrez RA, Orozco R, Halasa YA, Undurraga EA, Hamadeh RR, Hamidi S, Handal AJ, Hankey GJ, Hao Y, Harikrishnan S, Haro JM, Hernández-Llanes NF, Hoek HW, Hoek HW, Horino M, Horita N, Hosgood HD, Hoy DG, Hsairi M, Hu G, Husseini A, Huybrechts I, Iburg KM, Idrisov BT, Kwan GF, Ileanu BV, Pana A, Kawakami N, Shibuya K, Jacobs TA, Jacobsen KH, Jahanmehr N,

Jakovljevic MB, Jansen HAF, Jassal SK, Stein MB, Javanbakht M, Jayaraman SP, Jayatilleke AU, Jee SH, Jeemon P, Jonas JB, Kabir Z, Kalkonde Y, Kamal R, She J, Kan H, Karch A, Karimkhani C, Kaul A, Kazi DS, Keiyoro PN, Parry CD, Parry CD, Kengne AP, Matzopoulos R, Wiysonge CS, Stein DJ, Keren A, Khader YS, Khan EA, Khan G, Khang YH, Won S, Khera S, Tavakkoli M, Khoja TAM, Khubchandani J, Kim C, Kim D, Kimokoti RW, Kokubo Y, Koul PA, Koyanagi A, Kravchenko M, Varakin YY, Kuate B, Kuchenbecker RS, Kucuk B, Kuipers EJ, Lallukka T, Lallukka T, Meretoja TJ, Meretoja TJ, Latif AA, Lawrynowicz AEB, Leasher JL, Levi M, Li X, Liang J, Lloyd BK, Logroscino G, Lunevicius R, Pope D, Mahdavi M, Malta DC, Marcenes W, Matsushita K, Nachega JB, Tran BX, Nachega JB, Tran BX, Tedla BA, Memish ZA, Tedla BA, Mensink GBM, Mhimbira FA, Miller TR, Mills EJ, Miller TR, Mohammadi A, Mola GLD, Monasta L, Morawska L, Norman RE, Mori R, Mozaff D, Shi P, Werdecker A, Mueller UO, Paternina AJ, Westerman R, Paternina AJ, Seedat S, Naheed A, Nangia V, Nassiri N, Nguyen QL, Nkamedjie PM, Norheim OF, Norrving B, Nyakarahuka L, Obermeyer CM, Ogbo FA, Oh I, Oladimeji O, Sartorius B, Olusanya BO, Olivares PR, Olusanya JO, Opio JN, Oren E, Ortiz A, Ota E, Mahesh PA, Park E, Patel T, Patil ST, Patten SB, Wang J, Pereira DM, Cortinovis M, Giussani G, Perico N, Remuzzi G, Pesudovs K, Phillips MR, Remuzzi G, Pillay JD, Plass D, Tobollik M, Polinder S, Pond CD, Pope CA, Prasad NM, Qorbani M, Prasad NM, Radfar A, Rafay A, Rana SM, Rahman M, Rahman SU, Rajsic S, Rai RK, Raju M, Ranganathan K, Refaat AH, Rehm CD, Ribeiro AL, Rojas-Rueda D, Roy A, Satpathy M, Tandon N, Rothenbacher D, Saleh MM, Sanabria JR, Sanchez-Riera L, Sanabria JR, Sanchez-Niño MD, SarmientoSuarez R, Sawhney M, Schmidhuber J, Schneider IJC, Schutte AE, Silva DAS, Shahraz S, Shin M, Shaheen A, Shaikh MA, Sharma R, Shigematsu M, Shigematsu M, Yoon S, Shishani K, Sigfusdottir ID, Singh PK, Silveira DGA, Silverberg JI, Yano Y, Soneji S, Stranges S, Steckling N, Sreeramareddy CT, Stathopoulou V, Stroumpoulis K, Sunguya BF, Stroumpoulis K, Swaminathan S, Sykes BL, TabarésSeisdedos R, Talongwa RT, Tanne D, Tuzcu EM, Tanne D, Thakur J, Shaddick G, Thomas ML, Thrift AG, Thurston GD, Thomson AJ, Topor-Madry R, Topouzis F, ToporMadry R, Towbin JA, Uthman OA, Tobe-Gai R, Towbin JA, Tsilimparis N, Tsala Z, Tyrovolas S, Ukwaja KN, van Os J, Tsala Z, Vasankari T, Venketasubramanian N, Violante FS, Waller SG, Uneke CJ, Wang Y, Weichenthal S, Woolf AD, Xavier D, Xu G, Yakob B, Yip P, Kesavachandran CN, Montico M, Ronfani L, Yu C, Zaidi Z, Yu C, Yonemoto N, Younis MZ, Wubshet M, Zaidi Z, Zuhlke LJ, Zaki ME, Zhu J, Global, regional, and national comparative risk assessment of 79 behavioural, environmental and occupational, and metabolic risks or clusters of risks, 1990–2015: a systematic analysis for the Global Burden of Disease Study 2015, Lancet. 388 (2016) 1659–1724. doi:10.1016/S0140-6736(16)31679-8. [PubMed: 27733284]

[6]. CDC, What Are the Risk Factors for Lung Cancer?, Www.Cdc.Gov. (2017).

[7]. Veljkovic E, Jiricny J, Menigatti M, Rehrauer H, Han W, Chronic exposure to cigarette smoke condensate in vitro induces epithelial to mesenchymal transition-like changes in human bronchial epithelial cells, BEAS-2B, Toxicol. Vitr 25 (2011) 446–453. doi:10.1016/j.tiv.2010.11.011.

[8]. Zhang L, Gallup M, Zlock L, Basbaum C, Finkbeiner WE, McNamara NA, Cigarette smoke disrupts the integrity of airway adherens junctions through the aberrant interaction of p120-catenin with the cytoplasmic tail of MUC1, J. Pathol 229 (2013) 74–86. doi:10.1002/path.4070. [PubMed: 22833523]

[9]. Murthy VH, E-Cigarette Use Among Youth and Young Adults: A Report of the Surgeon General, 2016.

[10]. Behar RZ, Davis B, Wang Y, Bahl V, Lin S, Talbot P, Identification of toxicants in cinnamon-flavored electronic cigarette refill fluids, Toxicol. Vitr 28 (2014) 198–208. doi:10.1016/j.tiv.2013.10.006.

[11]. Bahl V, Lin S, Xu N, Davis B, Wang YH, Talbot P, Comparison of electronic cigarette refill fluid cytotoxicity using embryonic and adult models, Reprod. Toxicol 34 (2012) 529–537. doi:10.1016/j.reprotox.2012.08.001. [PubMed: 22989551]

[12]. Tommasi S, Bates SE, Behar RZ, Talbot P, Besaratinia A, Limited mutagenicity of electronic cigarettes in mouse or human cells in vitro, Lung Cancer. 112 (2017) 41–46. doi:10.1016/j.lungcan.2017.07.035. [PubMed: 29191599]

[13]. Thorne D, Crooks I, Hollings M, Seymour A, Meredith C, Gaca M, The mutagenic assessment of an electronic-cigarette and reference cigarette smoke using the Ames assay in strains TA98 and

TA100, Mutat. Res. - Genet. Toxicol. Environ. Mutagen 812 (2016) 29–38. doi:10.1016/j.mrgentox.2016.10.005.

[14]. Canistro D, Vivarelli F, Cirillo S, Marquillas CB, Buschini A, Lazzaretti M, Marchi L, Cardenia V, Rodriguez-Estrada MT, Lodovici M, Cipriani C, Lorenzini A, Croco E, Marchionni S, Franchi P, Lucarini M, Longo V, Della Croce CM, Vornoli A, Colacci A, Vaccari M, Sapone A, Paolini M, E-cigarettes induce toxicological effects that can raise the cancer risk, Sci. Rep 7 (2017) 1–9. doi:10.1038/s41598-017-02317-8. [PubMed: 28127051]

[15]. Lee H-W, Park S-H, Weng M, Wang H-T, Huang WC, Lepor H, Wu X-R, Chen L-C, Tang M, E-cigarette smoke damages DNA and reduces repair activity in mouse lung, heart, and bladder as well as in human lung and bladder cells, Proc. Natl. Acad. Sci 115 (2018) E1560–E1569. doi:10.1073/pnas.1718185115. [PubMed: 29378943]

[16]. Carpenter AE, Jones TR, Lamprecht MR, Clarke C, Kang IH, Friman O, a Guertin D, Chang JH, a Lindquist R, Moffat J, Golland P, Sabatini DM, CellProfiler: image analysis software for identifying and quantifying cell phenotypes., Genome Biol. 7 (2006) R100. doi:10.1186/gb-2006-7-10-r100. [PubMed: 17076895]

[17]. Lin SC, Yip H, Phandthong R, Davis B, Talbot P, Evaluation of Dynamic Cell Processes and Behavior Using Video Bioinformatics Tools, in: Video Bioinforma., Springer, 2015: pp. 167–186. doi:10.1007/978-3-319-23724-4.

[18]. Otsu N, A Threshold Selection Method from Gray-Level Histograms, IEEE Trans. Syst. Man. Cybern 9 (1979) 62–66. doi:10.1109/TSMC.1979.4310076.

[19]. Heerboth S, Housman G, Leary M, Longacre M, Byler S, Lapinska K, Willbanks A, Sarkar S, EMT and tumor metastasis, Clin. Transl. Med 4 (2015) 6. doi:10.1186/s40169-015-0048-3. [PubMed: 25852822]

[20]. Popper HH, Progression and metastasis of lung cancer, Cancer Metastasis Rev. 35 (2016) 75–91. doi:10.1007/s10555-016-9618-0. [PubMed: 27018053]

[21]. Stratton K, Kwan LY, Eaton DL, Health P, Practice PH, Division M, Public Health Consequences of E-Cigarettes, 2018. doi:10.17226/24952.

[22]. Behar RZ, Bahl V, Wang Y, Lin S, Xu N, Davis B, Talbot P, A method for rapid doseresponse screening of environmental chemicals using human embryonic stem cells, J. Pharmacol. Toxicol. Methods 66 (2012) 238–245. doi:10.1016/j.vascn.2012.07.003. [PubMed: 22820057]

[23]. Behar RZ, Luo W, Lin SC, Wang Y, Valle J, Pankow JF, Talbot P, Distribution, quantification and toxicity of cinnamaldehyde in electronic cigarette refill fluids and aerosols, Tob. Control 25 (2016) ii94–ii102. doi:10.1136/tobaccocontrol-2016-053224. [PubMed: 27633763]

[24]. Behar RZ, Luo W, Mcwhirter KJ, Pankow JF, Talbot P, Analytical and toxicological evaluation of flavor chemicals in electronic cigarette refill fluids, Sci. Rep 8 (2018) 1–11. doi:10.1038/s41598-018-25575-6. [PubMed: 29311619]

[25]. Wu Q, Jiang D, Minor M, Chu HW, Electronic cigarette liquid increases inflammation and virus infection in primary human airway epithelial cells, PLoS One. 9 (2014). doi:10.1371/journal.pone.0108342.

[26]. Lerner CA, Sundar IK, Yao H, Gerloff J, Ossip DJ, McIntosh S, Robinson R, Rahman I, Vapors produced by electronic cigarettes and E-juices with flavorings induce toxicity, oxidative stress, and inflammatory response in lung epithelial cells and in mouse lung, PLoS One. 10 (2015) 1–26. doi:10.1371/journal.pone.0116732.

[27]. Lerner CA, Rutagarama P, Ahmad T, Sundar IK, Elder A, Rahman I, Electronic cigarette aerosols and copper nanoparticles induce mitochondrial stress and promote DNA fragmentation in lung fibroblasts, Biochem. Biophys. Res. Commun. 477 (2016) 620–625. doi:10.1016/j.bbrc.2016.06.109.Electronic. [PubMed: 27343559]

[28]. Madsen LR, Krarup NHV, Bergmann TK, Brentzen S, Neghabat S, Duval L, Knudsen ST, A cancer that went up in smoke pulmonary reaction to e-cigarettes imitating metastatic cancer, Chest. 149 (2016) e65–e67. doi:10.1016/j.chest.2015.09.003. [PubMed: 26965975]

[29]. Kam Y, Quaranta V, Cadherin-bound β-catenin feeds into the Wnt pathway upon adherens junctions dissociation: Evidence for an intersection between β-catenin pools, PLoS One. 4 (2009). doi:10.1371/journal.pone.0004580.

[30]. Reynolds AB, Epithelial organization: New perspective on α-catenin from an ancient source, Curr. Biol 21 (2011) R430–R432. doi:10.1016/j.cub.2011.04.043. [PubMed: 21640901]

[31]. Goldstraw P, Chansky K, Crowley J, Rami-Porta R, Asamura H, Eberhardt WEE, Nicholson AG, Groome P, Mitchell A, Bolejack V, Ball D, Beer DG, Beyruti R, Detterbeck F, Eberhardt WEE, Edwards J, Galateau-Sallé F, Giroux D, Gleeson F, Huang J, Kennedy C, Kim J, Kim YT, Kingsbury L, Kondo H, Krasnik M, Kubota K, Lerut A, Lyons G, Marino M, Marom EM, Van Meerbeeck J, Nakano T, Nowak A, Peake M, Rice T, Rosenzweig K, Ruffini E, Rusch V, Saijo N, Van Schil P, Sculier JP, Shemanski L, Stratton K, Suzuki K, Tachimori Y, Thomas CF, Travis W, Tsao MS, Turrisi A, Vansteenkiste J, Watanabe H, Wu YL, Baas P, Erasmus J, Hasegawa S, Inai K, Kernstine K, Kindler H, Krug L, Nackaerts K, Pass H, Rice D, Falkson C, Filosso PL, Giaccone G, Kondo K, Lucchi M, Okumura M, Blackstone E, Abad Cavaco F, Ansótegui Barrera E, Abal Arca J, Parente Lamelas I, Arnau Obrer A, Guijarro Jorge R, Bascom GK, Blanco Orozco AI, González Castro M, Blum MG, Chimondeguy D, Cvijanovic V, Defranchi S, De Olaiz Navarro B, Escobar Campuzano I, Macía Vidueira I, Fernández Araujo E, Andreo García F, Fong KM, Francisco Corral G, Cerezo González S, Freixinet Gilart J, García Arangüena L, García Barajas S, Girard P, Goksel T, González Budiño MT, González Casaurrán G, Gullón Blanco JA, Hernández Hernández J, Hernández Rodríguez H, Herrero Collantes J, Iglesias Heras M, Izquierdo Elena JM, Jakobsen E, Kostas S, León Atance P, Núñez Ares A, Liao M, Losanovscky M, Lyons G, Magaroles R, De Esteban Júlvez L, Mariñán Gorospe M, McCaughan B, Kennedy C, Melchor Íñiguez R, Miravet Sorribes L, Naranjo Gozalo S, Álvarez De Arriba C, Núñez Delgado M, Padilla Alarcón J, Peñalver Cuesta JC, Park JS, Pass H, Pavón Fernández MJ, Rosenberg M, Ruffini E, Rusch V, Sánchez JS Escuín De Cos, Saura Vinuesa A, Serra Mitjans M, Strand TE, Subotic D, Swisher S, Terra R, Thomas C, Tournoy K, Van Schil P, Velasquez M, Wu YL, Yokoi K, The IASLC lung cancer staging project: Proposals for revision of the TNM stage groupings in the forthcoming (eighth) edition of the TNM Classification for lung cancer, J. Thorac. Oncol 11 (2016) 39–51. doi:10.1016/j.jtho.2015.09.009. [PubMed: 26762738]

[32]. Mcneill A, Brose LS, Calder R, Hitchman SC, Hajek P, H M, E-cigarettes: an evidence update A report commissioned by Public Health England, 2015 www.gov.uk/government/uploads/system/uploads/attachment_data/file/454516/Ecigarettes_an_evidence_update_A_report_commissioned_by_Public_Health_England.pdf.

[33]. Goniewicz ML, Knysak J, Gawron M, Kosmider L, Sobczak A, Kurek J, Prokopowicz A, Jablonska-Czapla M, Rosik-Dulewska C, Havel C, Jacob P, Benowitz N, Levels of selected carcinogens and toxicants in vapour from electronic cigarettes, Tob. Control 23 (2014) 133–139. doi:10.1136/tobaccocontrol-2012-050859. [PubMed: 23467656]

[34]. Zou W, Zou Y, Zhao Z, Li B, Ran P, Nicotine-induced epithelial-mesenchymal transition via Wnt/β-catenin signaling in human airway epithelial cells, Am. J. Physiol. Cell. Mol. Physiol 304 (2013) L199–L209. doi:10.1152/ajplung.00094.2012.

[35]. Dasgupta P, Rizwani W, Pillai S, Kinkade R, Kovacs M, Banerjee S, Carless M, Kim E, Coppola D, Nicotine induces cell proliferation, invasion and epithelial- mesenchymal transition in a variety of human cancer cell lines, Int. J. Cancer 124 (2009) 36–45. doi:10.1002/ijc.23894. [PubMed: 18844224]

[36]. Grando SA, Connections of nicotine to cancer, Nat. Rev. Cancer 14 (2014) 419–429. doi: 10.1038/nrc3725. [PubMed: 24827506]

[37]. Behar RZ, Hua M, Talbot P, Puffing topography and nicotine intake of electronic cigarette users, PLoS One. 10 (2015) 1–18. doi:10.1371/journal.pone.0117222.

[38]. Etter JF, Electronic cigarettes: A survey of users, BMC Public Health. 10 (2010). doi: 10.1186/1471-2458-10-231.

[39]. Brune K, Frank J, Schwingshackl A, Finigan J, Sidhaye VK, Pulmonary epithelial barrier function: some new players and mechanisms, Am. J. Physiol. - Lung Cell. Mol. Physiol 308 (2015) L731–L745. doi:10.1152/ajplung.00309.2014. [PubMed: 25637609]

Highlights:

- EC exposure caused an epithelial-to-mesenchymal transition (EMT) of lung cancer cells
- E-cadherin was lost from cell junctions and cells did not adhere to each other
- Active β-catenin was translocated from the cell surface to the nucleus
- Motility and directed movement increased in cells undergoing an EMT
- EC use may contribute to cancer progression for those at risk for lung cancer

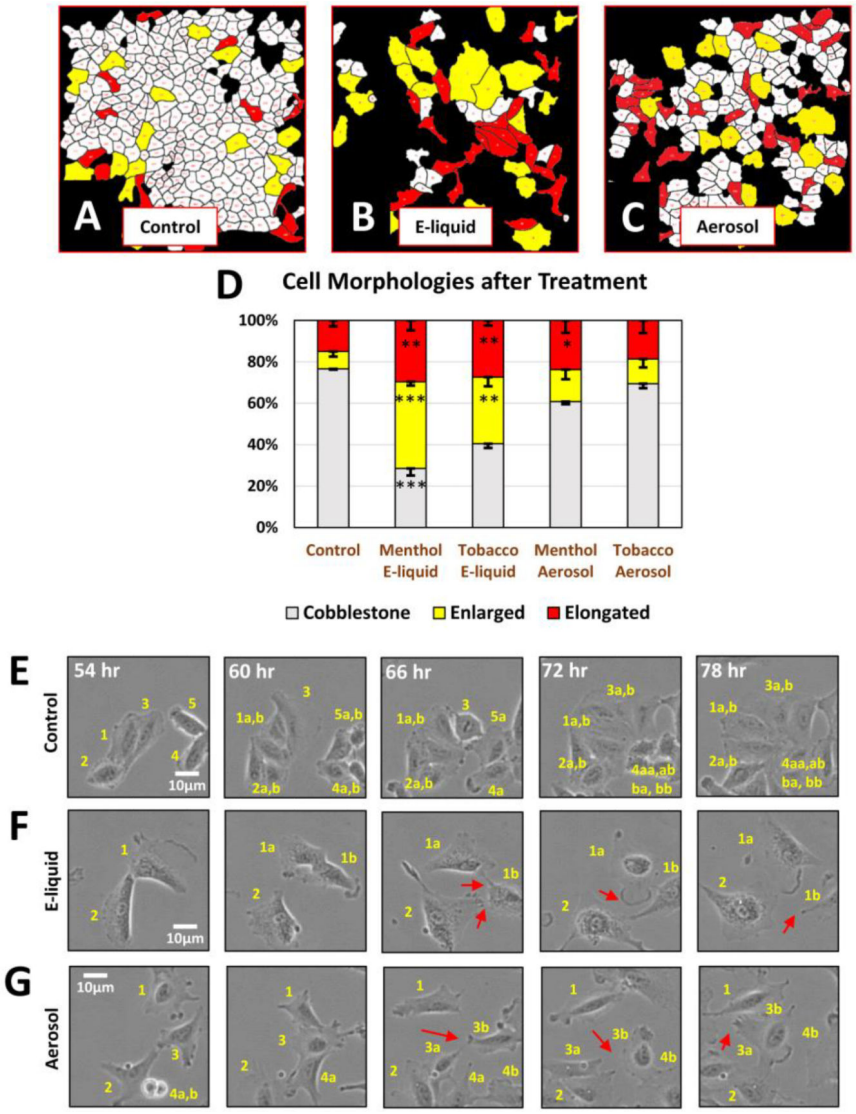

Figure 1: A549 Cell Morphology after EC Treatment.

(A-C) Control A549 cells and cells treated 3–4 days with e-liquid and aerosol were image processed to quantify the percent of cobblestone (white), enlarged (yellow), and elongated (red) morphologies. (D) E-liquid and aerosol treatment decreased the cobblestone and increased the elongated (mesenchymal-like) sub-populations. Each error bar is the mean ± standard error of the mean (SEM) of three independent experiments. Statistical analysis was done on arcsine transformed data using a one-way ANOVA with Dunnett's post hoc test. (E-G) Film-strips show that control cells adhered with neighbors, while treated cells failed to adhere. Individual cells are labeled numerically and then labeled with an additional "a" and "b" to denote daughter cells produced by division. Red arrows point to loss of tight junction.

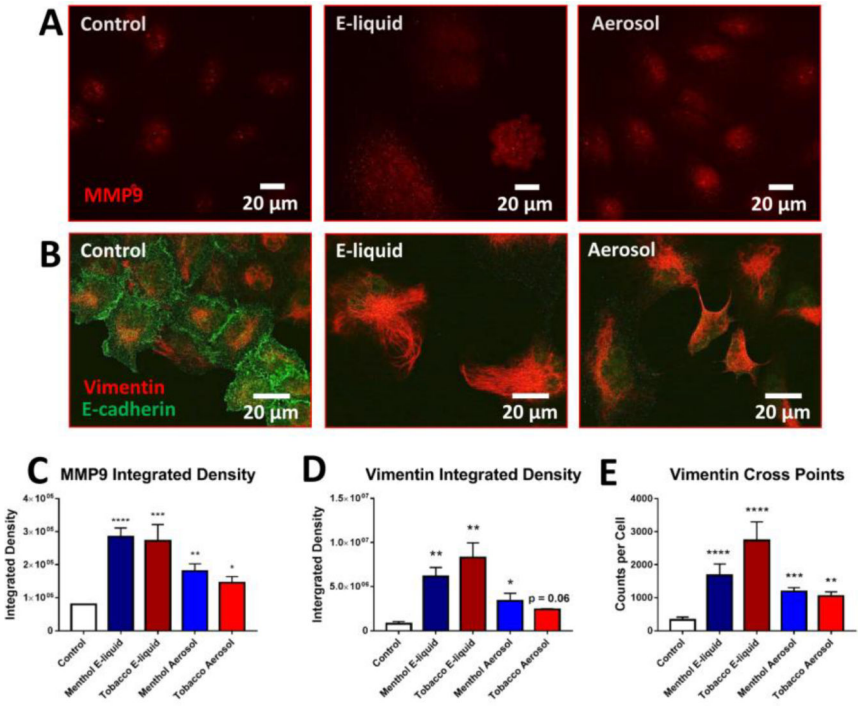

Figure 2: Upregulation of EMT Markers in E-liquid and Aerosol Treated Cells.

(A) Immunofluorescence of 4-day treated A549 cells labeled with MMP9 antibody. (B) Immunofluorescence of 8-day treated A549 cells co-labeled with E-cadherin and vimentin antibodies. (C) Quantification of integrated density (total area x mean intensity) of MMP9 fluorescent images. Each error bar is the mean ± SEM of three independent experiments. (D-E) Integrated density and cross points of vimentin fluorescent images. Increase of integrated density and cross points are indicative of increased protein expression. Each error bar is the mean ± SEM of five independent experiments. One-way ANOVAs with Dunnett's post hoc test were performed on natural log transformed data. Asterisks on top of each bar indicate the statistical significance. (* = $p < 0.05$. ** = $p < 0.01$. *** = $p < 0.001$. **** = $p < 0.0001$)

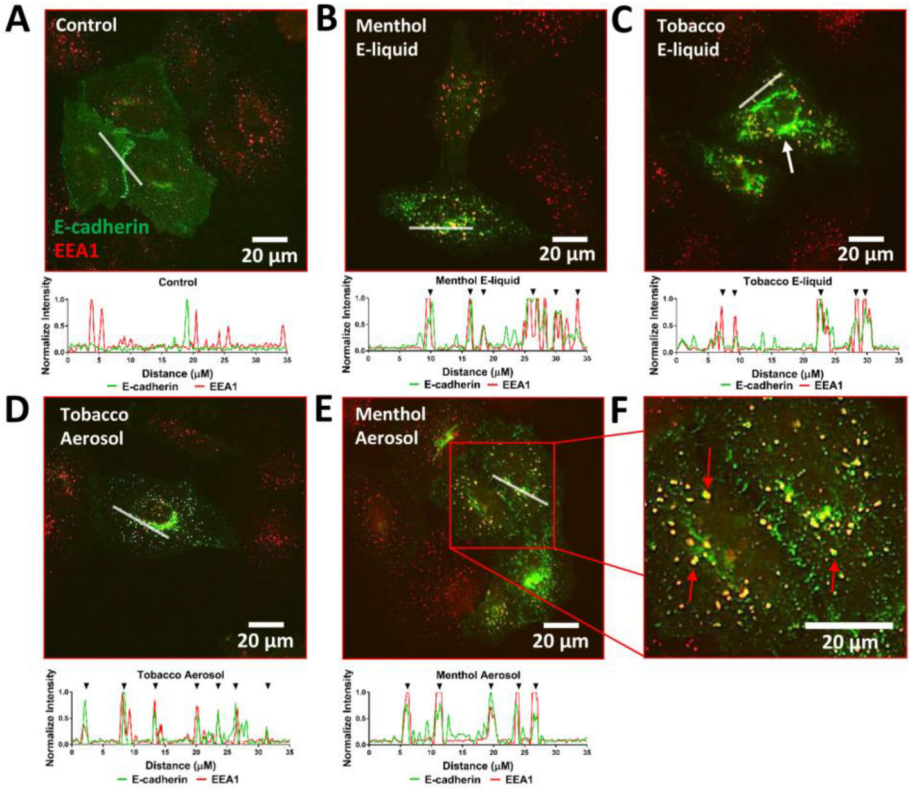

Figure 3: E-cadherin Internalization by Endocytosis.

(A-E) 4-day treated A549 cells were transfected with an E-cadherin plasmid and co-immuno-labelled with an EEA1 antibody to demonstrate internalization of E-cadherin. A line scanning method was used to do intensity profiling to confirm the co-localization of the E-cadherin and EEA1 signals. Black arrowheads above each graph (except control) show co-localization of the two channels. (F) Enlarged image of 4-day menthol aerosol treated cells. Red arrows show co-localization of E-cadherin and EEA1.

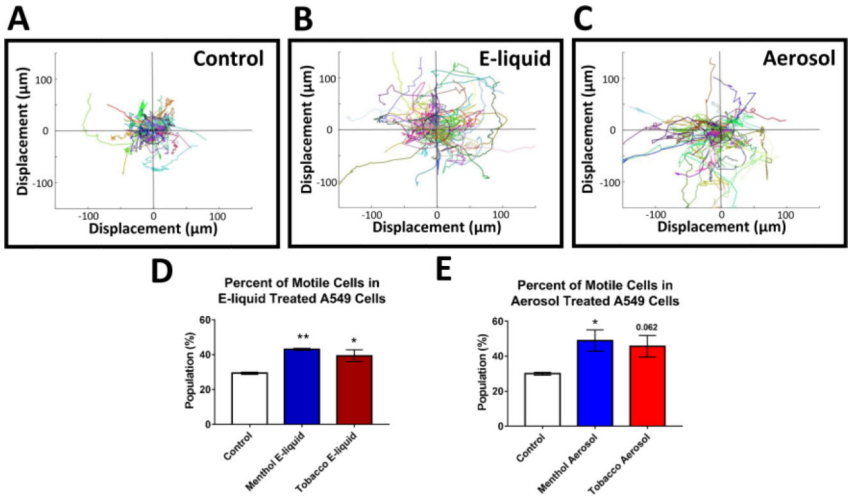

Figure 4: Increased Motility after EC Treatment

(A-C) Motility graphs show compilation of trajectories and distance traveled by individual control cells and treated cells (central circles are positioned 25µm from the starting location). Different colors correlate with different cells tracks. (D-E) The percent of "motile cells" (displacement > 25um) increased in treated groups. Each error bar is the mean ± SEM of four independent experiments. Motility data statistical analysis were done using a one-way ANOVA with Dunnett's post hoc test; treated groups were compared to the control. Asterisks on top of each bar indicate the statistical significance. (* = $p < 0.05$. ** = $p < 0.01$.)

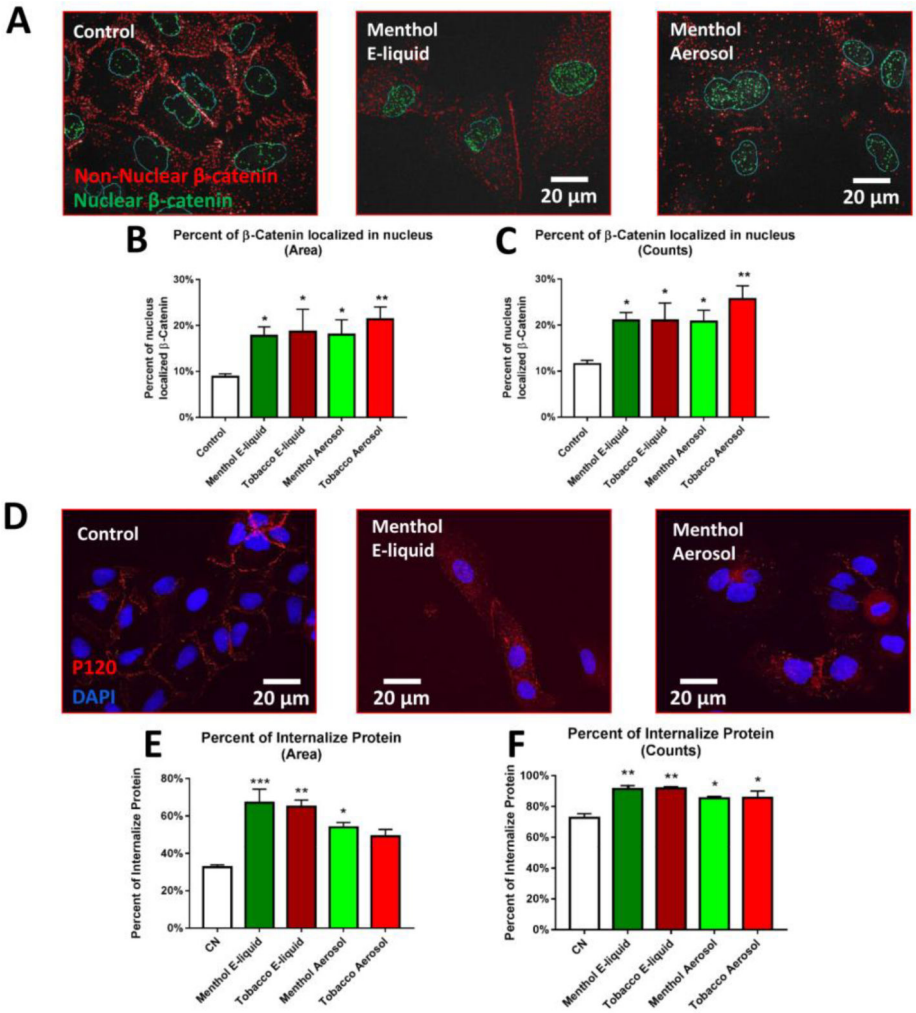

Figure 5: Translocation of Two Catenin-Family Transcription Factors.

(A) Active β-catenin in the nucleus (green) and cytoplasm (red) in segmented images. (B-C) Quantification of percent area and counts of active β-catenin puncta inside the nucleus. Each error bar is the mean ± SEM of six independent experiments. One-way ANOVA with Dunnett's post hoc test was performed on B and C arcsine-transformed percent data; treated groups were compared to the control. (D) 8-day treated A549 cells immunolabeled with P120. (E-F) Quantification of the percent area and counts of internalized P120. Each error bar is the mean ± SEM of three independent experiments. One-way ANOVA with Dunnett's post hoc test was performed on E and F. Asterisks on top of each bar indicate the statistical significance. (* = $p < 0.05$. ** = $p < 0.01$. *** = $p < 0.001$.).